

Production and Decay of the $\phi(1680)$ in $\pi^+d \rightarrow pp\pi^+\pi^-\pi^0$ at 6.95 GeV/c

J. A. J. Matthews†, J. D. Prentice, and T. S. Yoon
University of Toronto, Toronto 5, Ontario, Canada

and

J. T. Carroll, M. W. Firebaugh, and W. D. Walker
University of Wisconsin, Madison, Wisconsin 53706

(Received 2 December 1970)

An analysis of the 1.68-GeV mass region of the $m(\pi^+\pi^-\pi^0)$ spectrum in our $\pi^+d \rightarrow pp\pi^+\pi^-\pi^0$ data confirms the existence of an $I^G = 0^-$ enhancement at this mass, the $\phi(1680)$, which is distinct from the $I=1 A_3$ meson. This resonance was found to decay preferentially into $\rho\pi$ with a $3\pi/(3\pi+\rho\pi)$ branching ratio of <30%. A spin-parity analysis of the $\phi(1680)$ favors $J^P = 1^-, 2^+, 3^-$ for spins ≤ 3 , although $J^P = 1^+, 2^-$ cannot be rigorously excluded. The mass and favored natural spin-parity of the $\phi(1680)$ suggest that it may be the Regge recurrence of the ω^0 meson. Assuming a natural-spin-parity assignment, the decay angular distributions of the $\phi(1680)$ suggest that there exists a contribution from unnatural-parity exchange in the production mechanism. The t dependence of the differential cross section and the energy dependence of the total cross section for $\pi^+n \rightarrow \phi(1680)p$ were found to be similar to those of $\pi^+n \rightarrow (\omega^0, A_3^0)p$ also seen in the data. As with these latter processes, the energy dependence of the cross section for $\pi^+n \rightarrow \phi(1680)p$ cannot be explained by simple ρ Regge exchange. The $I=1 f^0\pi^0$ cross section in the A_3^0 mass region was found to be small, and suggests that the production cross section of the A_3 meson by charge exchange is significantly less than that observed in non-charge-exchange reactions such as $\pi^-p \rightarrow A_3^-p$.

I. INTRODUCTION

Evidence is accumulating^{1,2} for the existence of an $I^G = 0^-$ state in the mass region 1.650–1.700 GeV. This enhancement is observed in the channel $\pi^+n \rightarrow (\pi^+\pi^-\pi^0)p$, and has tentatively been named the $\phi(1670)$.² This state is distinct from the A_3 meson which has $I^G = 1^-$ and a somewhat lower mass.³ The state $\phi(1680)$ is found at a mass of ~ 1.680 GeV in our data and will be referred to as the “ $\phi(1680)$ ” in the present paper.

Recent evidence for possible 5π decay modes of the A_3 or $\phi(1680)$ comes from a $\bar{p}p$ annihilation experiment⁴ and Kp experiments^{5,6} where enhancements in the $\omega^0\pi^+\pi^-$ mass distributions were observed in the A_3 - $\phi(1680)$ mass region. Since the status of the A_3 as a resonance is uncertain at the present time,⁷ an improved understanding of the $\phi(1680)$ should help in resolving this problem.

Data at 6.95 GeV/c have been analyzed to determine the properties of this resonance observed in $\pi^+d \rightarrow pp\phi(1680)$ with $\phi(1680) \rightarrow \pi^+\pi^-\pi^0$. Mass, width, and cross-section measurements are presented in Sec. III. This is followed in Sec. IV by a determination of the differential cross section for $\phi(1680)$ production which appears to be qualitatively similar to ω^0 and A_3^0 production also seen in this channel. The decay modes of the $\phi(1680)$ are analyzed in Sec. V and strongly favor an $I=0$ assignment for this resonance in agreement with previous analy-

ses.^{1,2} A spin-parity analysis of the 3π Dalitz plot, restricted to $I=0$ states, has been presented elsewhere,⁸ but will be sketched in Sec. VI for completeness. This analysis⁸ favored the natural-spin-parity series $J^P = 1^-, 2^+, 3^-$ for the $\phi(1680)$ over $J^P = 1^+$ and 2^- . Spin-parities $J^P = 0^-$ and 3^+ had probabilities <1% and were considered unlikely. The angular distribution of the normal to the 3π decay plane is fitted in Sec. VI and suggests, assuming a natural-spin-parity assignment for the $\phi(1680)$, that there exists a contribution from unnatural-parity exchange in the production amplitude. Finally, the energy dependence for the production of $\phi(1680)$ and A_3 is discussed in Sec. VII.

II. EXPERIMENTAL DETAILS

The data to be discussed come from a 650 000-picture exposure in the ANL-MURA 30-in. deuterium bubble chamber to π^+ mesons at 6.95 GeV/c. Approximately 30 000 three- and four-prong events selected with one and two identifiable protons, respectively, have been processed through the Maryland version of BRAVE-TVGP-SQUAW programs to yield a final sample of 5471 events in the channel

$$\pi^+d \rightarrow pp\pi^+\pi^-\pi^0. \quad (1)$$

All events are consistent with scan-table ionization estimates. Events of the type $\pi^+n \rightarrow p\pi^+\pi^-\pi^0$

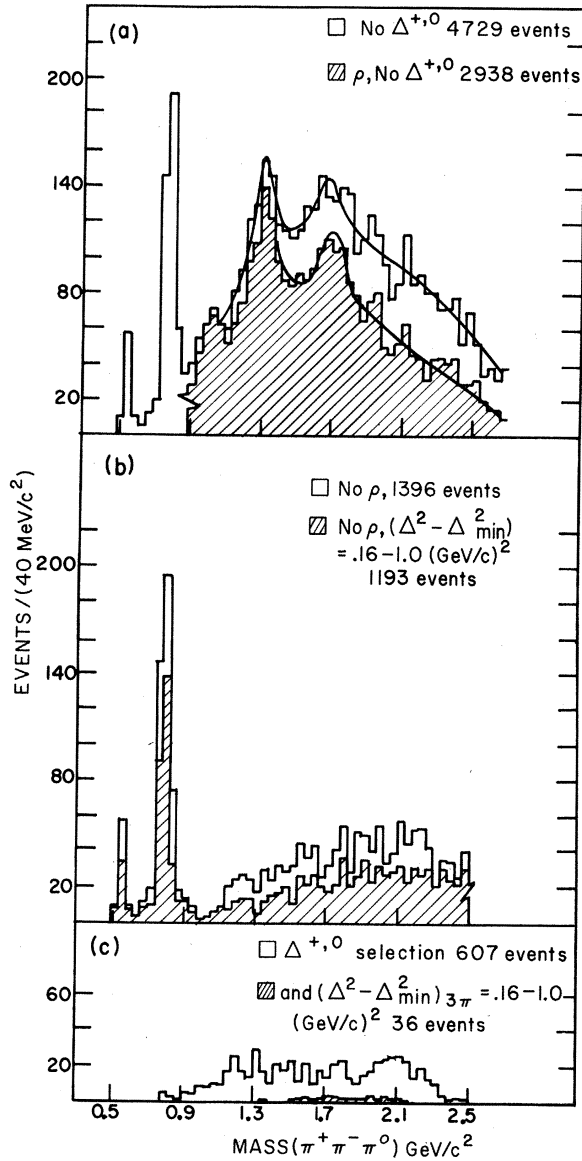


FIG. 1. (a) $\pi^+\pi^-\pi^0$ mass distributions for reaction (1). Events with $\Delta^{+,0}$ have been excluded as discussed in the text, Sec. III. The curves are fits of Breit-Wigner functions plus polynomially modified phase space as described in Sec. III. Significant enhancements are seen at the η^0 (550), ω^0 (784), A_2^0 (1310), and ϕ (1680). (b) $\pi^+\pi^-\pi^0$ mass distributions for those events outside the ρ bands. (c) $\pi^+\pi^-\pi^0$ mass distributions for those events having a $(p\pi)^{+,0}$ mass in the $\Delta^{+,0}$ mass interval, and with $|t|_{n \rightarrow (p\pi)} < 0.1$ (GeV/c)².

were preferentially selected by requiring a spectator momentum < 300 MeV/c for four-prong events, and by requiring that the projection of the reconstructed spectator momentum in the plane perpendicular to the camera axes be less than 100 MeV/c for three-prong events. The events used have kinematic reconstruction probabilities $\geq 5\%$.

The combined three- and four-prong data have been used in the analysis. All aspects of the analysis have been applied to the separate three- and four-prong samples, however, and have yielded equivalent results within errors.

III. MASS, WIDTH, AND CROSS SECTION FOR THE ϕ (1680)

The $\pi^+\pi^-\pi^0$ mass distributions are shown in Fig. 1. Strong production of $\Delta^{+,0}$ (1236) has necessitated the exclusion of events in the $(p\pi)^{+,0}$ mass interval $1.16 < m(p\pi) < 1.32$ GeV with $|t|_{n \rightarrow p\pi} < 0.1$ (GeV/c)². Utilization of these cuts effectively removed the majority of the peripherally produced $\Delta^{+,0}$ events [the ratio of the number of $\Delta^{+,0}$ events to the total number of $(p\pi)^{+,0}$ events with $|t| < 0.1$ (GeV/c)² was $> 80\%$] and yielded $(p\pi)^{+,0}$ mass distributions with a negligible number of events above background in the Δ (1236) mass region. The $\pi^+\pi^-\pi^0$ mass spectrum for the events excluded by this cut is shown in Fig. 1(c).

The 3π and $\rho\pi$ mass distributions shown in Fig. 1(a) have been fitted with a distribution of the form⁹

$$P(1 + \gamma_1 m + \gamma_2 m^2 + \gamma_3 m^3) \times \left(\gamma_0 + \sum_i \frac{\beta_i m_i \Gamma_i / \pi}{(m^2 - m_i^2)^2 + (m_i \Gamma_i)^2} \right),$$

where m is the 3π mass, the γ_i are parameters defining the background, the β_i are the normalization coefficients to the total number of events in the i th mass peak, and P is a sum of 3π and $\rho\pi$ phase space.¹⁰

The mass M and width Γ of the ϕ (1680) obtained from these fits were $M = 1.679 \pm 0.017$ GeV and $\Gamma = 0.155 \pm 0.020$ GeV, respectively. As a check on the reliability of these statistical errors, various subsets of the data were also fitted and the rms deviations calculated for the fitted masses and widths. The rms deviations in the mass and width were found to be $< \frac{1}{2}$ the statistical errors. The statistical fitting errors are quoted therefore as reasonable estimates in the uncertainties in these quantities. Allowances for a systematic mass shift have not been included in the error estimates.

The cross section for $\pi^+ n \rightarrow \phi(1680)p$ with the decay $\phi(1680) \rightarrow \pi^+\pi^-\pi^0$ was obtained from the integrated area under the Breit-Wigner function fitted to the ϕ (1680) mass peak. This yields a value of 33.5 ± 9.0 μb for the momentum transfer range $|t - t_{\min}|_{n \rightarrow p} < 1.0$ (GeV/c)².

As a check on the present fits to the 3π mass distribution, we find for the A_2^0 a mass $M = 1.310 \pm 0.009$ GeV, a width $\Gamma = 0.132 \pm 0.018$ GeV, and a cross section $\sigma = 54 \pm 15$ μb , in agreement with our previous analysis.¹¹

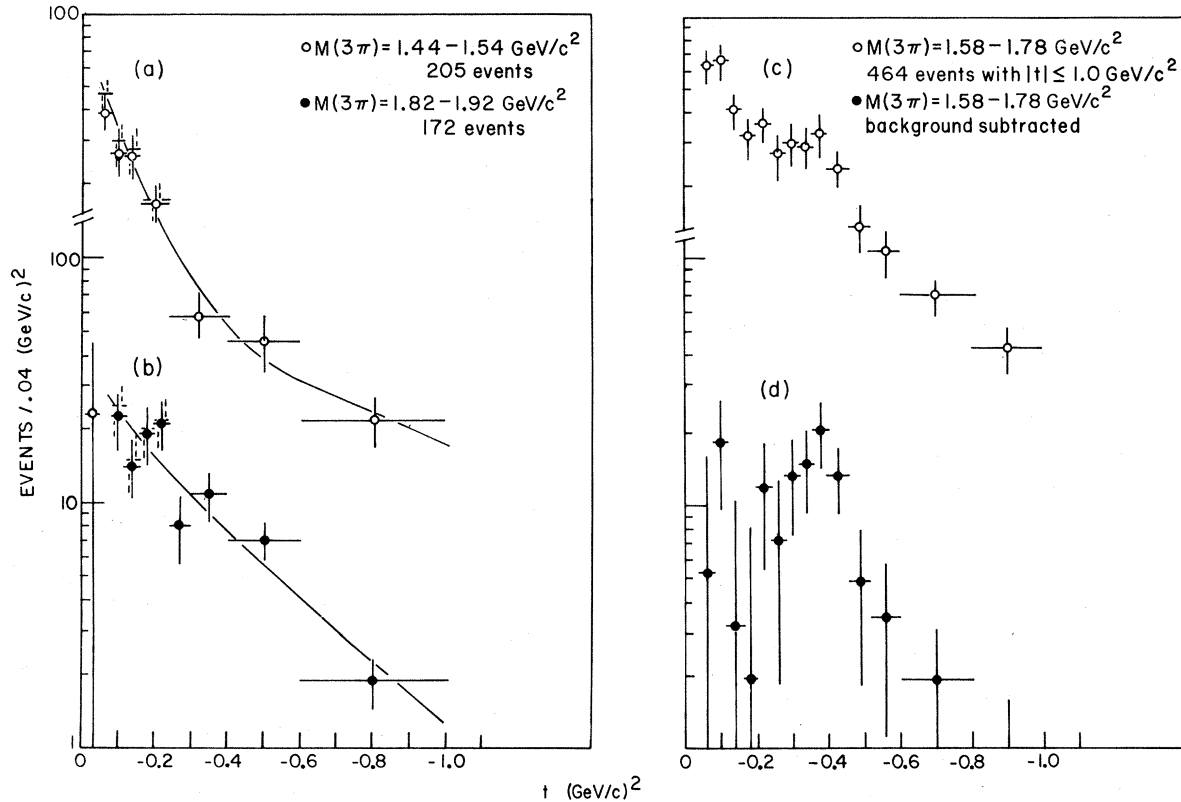


FIG. 2. (a) and (b) Differential cross sections for control regions below and above the $\phi(1680)$, respectively. The points with dashed error bars have been corrected for Pauli exclusion effects resulting from the use of a deuteron target. The curves are fits of two incoherent exponentials. (c) Differential cross section in the $\phi(1680)$ mass band, $1.58 \leq m(3\pi) \leq 1.78 \text{ GeV}$. (d) Differential cross section for the $\phi(1680)$ with background subtraction as described in Sec. IV.

IV. DIFFERENTIAL CROSS SECTION FOR THE $\phi(1680)$

The differential cross sections for the 3π mass regions at the $\phi(1680)$, $1.58 < m(3\pi) < 1.78 \text{ GeV}$, and in two control regions below and above the $\phi(1680)$ mass band, $1.44 < m(3\pi) < 1.54 \text{ GeV}$ and $1.82 < m(3\pi) < 1.92 \text{ GeV}$, respectively, are shown in Fig. 2. The differential cross section in the control regions have been corrected for 50% spin-flip at the nucleon¹² as shown dashed in Figs. 2(a) and 2(b). These corrected distributions have been fitted with two incoherently added exponential functions. The background in the $\phi(1680)$ band was then assumed to be described by a weighted average of these fitted distributions.

The differential cross section of the $\phi(1680)$, shown in Fig. 2(d), was obtained by subtracting the fitted background from the total differential cross section in the $\phi(1680)$ mass band, Fig. 2(c). The normalization was adjusted to the number of $\phi(1680)$ events determined from the 3π mass fits described in Sec. III. The errors include the statistical errors on each point and the over-all error

in the number of resonance events in the $\phi(1680)$ mass band. No allowance was made for the uncertainties in the fitted form of the background.

Within the limits of these assumptions and the large uncertainties on the points in Fig. 2(d), there is evidence for a distinct difference between the t dependence of the differential cross section for the $\phi(1680)$ and for the adjacent background regions. This subtraction suggests that the differential cross section for the $\phi(1680)$ in $\pi^+n \rightarrow \phi(1680)p$ has a flat or possibly decreasing t dependence towards the forward direction. A similar effect is seen in the differential cross sections for $\pi^+n \rightarrow \omega^0 p$ (Ref. 13) and $\pi^+n \rightarrow A_2^0 p$ (Ref. 14) from the same data.

If this is the case, the $\phi(1680)$ enhancement should appear more prominently in the 3π data at t values somewhat removed from t_{\min} .¹⁵ This is confirmed in Fig. 3. The 3π and $\rho\pi$ distributions, as in Fig. 1, have been plotted for events with $t' = t - t_{\min}$ in the range $-0.16 > t' > -1.0 \text{ (GeV}/c)^2$. These distributions have been fitted following procedures similar to those of Sec. III, and have yielded masses and widths for the $\phi(1680)$ in good agreement with the previous values. The number of

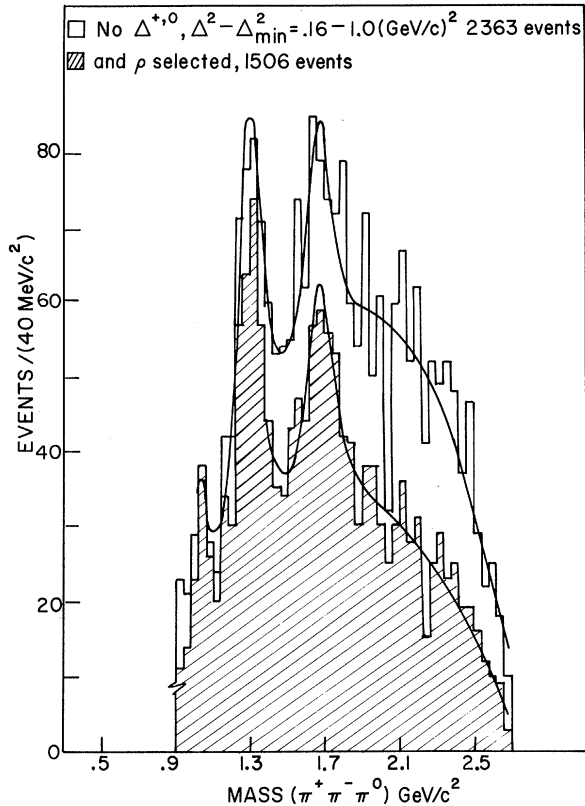


FIG. 3. $\pi^+\pi^-\pi^0$ mass distribution for reaction (1). Events lie in the t' range $0.16 \leq |t - t_{\min}|_{\pi \rightarrow 3\pi} \leq 1.0$ $(\text{GeV}/c)^2$. The curves are fits of Breit-Wigner functions plus polynomially modified phase space.

events in the $\phi(1680)$ enhancement in the t' -cut data was $\sim(20 \pm 10)\%$ less than for the entire t region. This decrease in the number of events in the $\phi(1680)$ enhancement is consistent with the apparent drop in the forward direction of the $\phi(1680)$ differential cross section as shown in Fig. 2(d).

Use of this intermediate t' cut effectively removes the need for the $\Delta^{+,0}$ cut as shown by the cross-hatched data in Fig. 1(c). The $\Delta^{+,0}$ cut does not produce the dip in the differential cross section of Fig. 2(d), however, as can be seen by noting that there are no enhancements at the $\phi(1680)$ mass in the 3π data associated with $\Delta^{+,0}$ events as shown in Fig. 1(c). As an alternative check on this behavior, the differential cross section for the $\phi(1680)$ has also been evaluated for ρ selection alone, and is consistent with the ρ , no $\Delta^{+,0}$ data discussed above, and presented in Fig. 2.

V. THREE-PION DECAY MODES OF THE $\phi(1680)$

Fits to the 3π and $\rho\pi$ mass distributions, as described in Sec. III, were consistent with a pure $\rho\pi$ decay mode for the $\phi(1680)$. At the present level of statistics, however, a branching ratio for

$[\phi(1680) \rightarrow \rho\pi] / [\phi(1680) \rightarrow (\rho\pi + 3\pi)] > 70\%$ would be indistinguishable from a pure $\rho\pi$ decay. The 3π data outside the ρ bands are shown in Fig. 1(b) for comparison.

The individual $\rho\pi$ mass distributions for ρ defined as $0.66 < m(2\pi) < 0.86$ GeV are shown in Figs. 4(a)–4(c), and in Figs. 4(d)–4(f) with the intermediate t' cut imposed as discussed in Sec. IV. Enhancements at the $\phi(1680)$ occur for each $\rho\pi$ combination. These enhancements remain, although with diminished significance, when only the $\rho\pi$ data outside the ρ -band overlap regions are plotted, as shown cross-hatched in Fig. 4. The enhancement at the $\phi(1680)$ in the $\rho^0\pi^0$ distribution cannot come from an $I=1$ state and suggests $I=0$ or 2 for this resonance.

In the $\phi(1680)$ mass band, $1.58 < m(3\pi) < 1.78$ GeV, there are approximately $(56 \pm 17):(69 \pm 18):(41 \pm 15)$ events above a smooth background in the channels $\rho^-\pi^+ : \rho^0\pi^0 : \rho^+\pi^-$, respectively. These amplitudes favor an $I=0$ assignment for the $\phi(1680)$, which satisfies the $I=0$ branching ratio 1:1:1 to within 1 standard deviation. For the $I=1$ or 2 assignments, however, the branching ratios are satisfied only within 3.9 and 2.5 standard deviations, respectively.

These conclusions would not necessarily apply if both $I=1$ and $I=2$ resonances occurred in this region. A recent result from a π^-d experiment¹⁶ at 7.0 GeV/c is consistent with there being no events above a smooth background in the $\pi^-\pi^-\pi^0$ or the $\rho^-\pi^-$ data in the $\phi(1680)$ mass region. Taking a 2-standard-deviation limit on the $I=2$ production in Ref. 16 yields $\sigma_{I=2}(\rho^-\pi^-) < 4 \mu\text{b}$. If the $I=2$ resonance were produced by $I=1$ exchange, the $I=2$ cross section in the $(\rho\pi)^0$ channel would be $< \frac{2}{3} \mu\text{b}$, and can be neglected in comparison to the $\phi(1680)$ cross section reported in Sec. III.

In order to confirm that the $\phi(1680)$ decays into all three $\rho\pi$ channels, the $\pi\pi$ mass distributions have been plotted in Fig. 5 for data with 3π masses in the two control regions and the $\phi(1680)$ mass region as defined in Sec. IV. These distributions were fitted in a manner similar to that described in Sec. III. Enhancements in the number of events in the ρ peaks were observed in all ρ charge states for $\pi\pi$ data from the $\phi(1680)$ mass band over $\pi\pi$ data from the combined control regions. This was consistent, therefore, with our previous isospin analysis.

Fits to the $\pi^+\pi^-$ mass distribution from 3π data in the $\phi(1680)$ mass band yield 40 ± 20 events in the f^0 peak, after correction for similar enhancements in the $\pi^-\pi^0$ and $\pi^+\pi^0$ mass distributions. Similarly, the number of f^0 events remaining in the ρ selected data, shown cross-hatched in Fig. 5, was 20 ± 10 events, or about 5% of the data in the $\phi(1680)$ mass

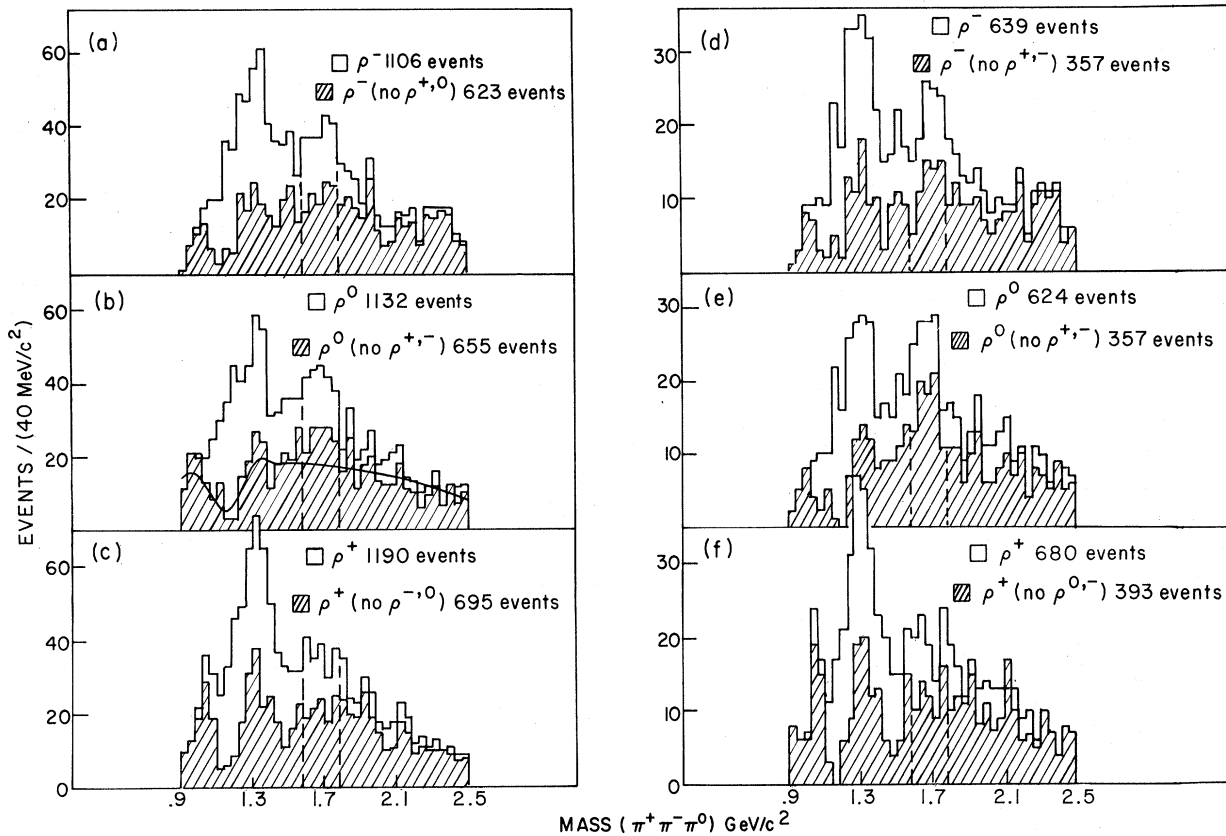


FIG. 4. (a) $m(\rho^-\pi^+)$, (b) $m(\rho^0\pi^0)$, (c) $m(\rho^+\pi^-)$ for data in the separate charged ρ bands. Dashed lines mark the $\phi(1680)$ mass band $1.58 \leq m(3\pi) \leq 1.78$ GeV/c^2 . The cross-hatched data excludes events in overlapping ρ bands. The curve on the $\rho^0\pi^0$ (no $\rho^{+,-}$) data was a fit of polynomially modified phase space to data outside the $\phi(1680)$ mass band. (d)–(f) are the same as (a)–(c) but with $0.16 \leq |t - t_{\min}|_{\pi \rightarrow 3\pi} \leq 1.0$ $(\text{GeV}/c)^2$.

band with ρ selected. This was confirmed by fits to the Dalitz plots in the ρ bands as described in Sec. VI.

The $f^0\pi^0$ mass distribution is plotted in Fig. 6(b). The cross section rises sharply at threshold, as has been observed in A_3^+ production in π^+p experiments^{17–20} and in the analogous $K^*(1420)\pi$ mass distribution in the L -meson mass region seen in Kp experiments.^{21, 22} When events in the $f^0\pi^0$, $\rho^+\pi^-$ overlapping bands are excluded, as shown in the cross-hatched data in Fig. 6(b), no significant enhancements remain in the $\phi(1680)$ region.

To aid in the interpretation of the $f^0\pi^0$ mass spectrum, the analogous “ $f^\pm\pi^\mp$ ” mass distributions have been plotted in Figs. 6(a), and 6(c) for “ f^\pm ” selected with $1.18 < m(\pi^+\pi^0) < 1.34$ GeV . Distributions were obtained that were similar to the $f^0\pi^0$ mass plot.

The similarities of the three “ f ” π mass distributions of Fig. 6 can be explained by noting that constructive interference in the overlapping ρ bands for an $I=0$ state decaying through $\rho\pi$ is reflected as enhancements in the “ f ” mass regions when

$m(3\pi) \sim 1.65$ GeV . Experimental evidence for an interference in the crossed bands is seen when the $\pi\pi$ mass distributions of Figs. 5(a) and 5(c) are compared for data lying in the $\phi(1680)$ mass band and for data coming from the two control regions. Enhancements are seen to exist above the fitted background in both the “pseudo- f^\pm ” mass regions for data having a 3π mass in the $\phi(1680)$ mass band.

This is confirmed quantitatively in the Dalitz-plot spin-parity analysis of Sec. VI, where spin-parity $J^P = 1^-$ is favored over $J^P = 2^+$ and 1^+ is favored over 2^- , for the $\phi(1680)$. The differences in the Dalitz-plot distributions for these cases are that spin-parities $J^P = 1^\pm$ have constructive interference in the overlapping ρ bands, whereas spin-parities $J^P = 2^\mp$ have destructive interference.²³

The similarity of the longitudinal-momentum distributions for the π^- and π^0 mesons in the data (not shown), considered with the similarity of the simplest multi-Regge diagrams applicable to this channel, suggests that “ $f^\pm\pi^\mp$ ” and $f^0\pi^0$ mass distributions should be similar, apart from resonant f^0 effects.²⁴ Attempting to obtain the “true” $f^0\pi^0$ mass

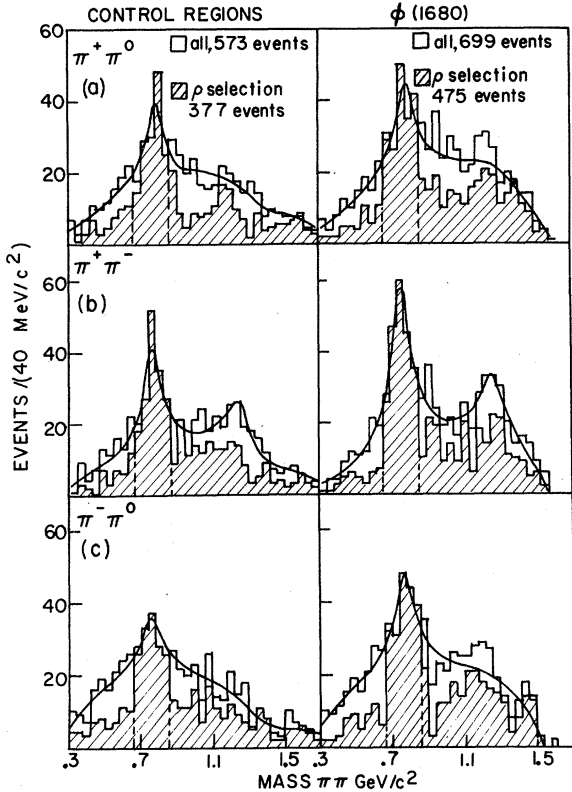


FIG. 5. (a) $m(\pi^+\pi^0)$, (b) $m(\pi^+\pi^-)$, (c) $m(\pi^-\pi^0)$, from data in the control regions below and above the $\phi(1680)$, $1.44 \leq m(3\pi) \leq 1.54$ GeV and $1.82 \leq m(3\pi) \leq 1.92$ GeV, respectively, plotted in the left-hand figures; and from data in the $\phi(1680)$ band $1.58 \leq m(3\pi) \leq 1.78$ GeV plotted in the right-hand figures. The cross-hatched data are events lying in the ρ bands. The curves are fits of Breit-Wigner functions plus polynomially modified phase space as discussed in Sec. VI.

distributions, the distributions in Figs. 6(a) and 6(b) have been subtracted to yield Fig. 7. No significant enhancements occur at the $\phi(1680)$. In fact, the resulting distribution possesses a phase-space-like distribution. The number of events remaining in the $\phi(1680)$ mass region of Fig. 7 was in agreement with the fitted number of f^0 events determined from Fig. 5(b).

VI. SPIN-PARITY ANALYSIS OF THE $\phi(1680)$

In the rest frame of the $\phi(1680)$, the decay $\phi(1680) \rightarrow 3\pi$ can be completely described (apart from an inessential rotation)²⁵ by the direction of the normal to the decay plane of the 3π 's and by two coordinates on the Dalitz plot. These distributions have been fitted for several spin-parity assignments for the $\phi(1680)$. Fits to the Dalitz plot in the $\phi(1680)$ mass band have been described elsewhere,⁸ but will be sketched here for completeness.

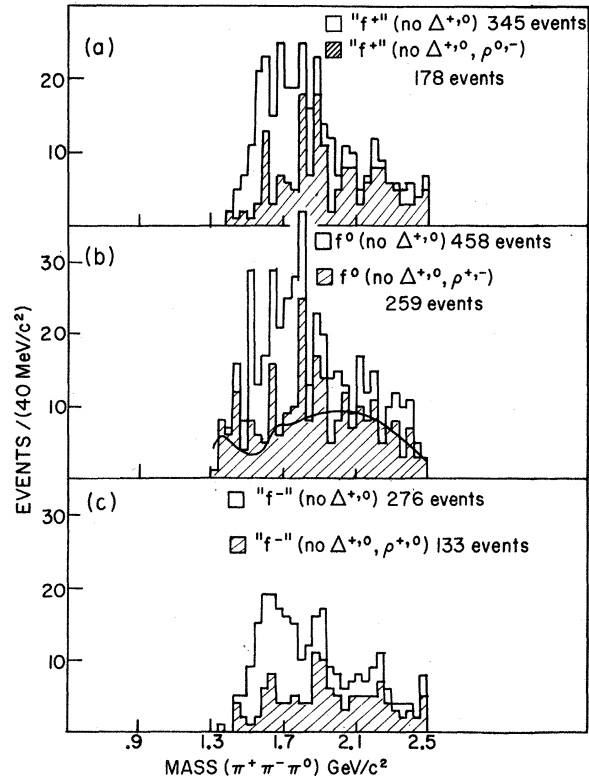


FIG. 6. (a) " $f^+\pi^-$ ", (b) $f^0\pi^0$, and (c) " $f^-\pi^+$ " mass distributions for data with $m(\pi\pi)$ in the f^0 mass band, $1.18 \leq m(\pi\pi) \leq 1.34$ GeV. The " f^+ " and " f^- " are analogous mass cuts to that used to select f^0 events. The cross-hatched data lie outside overlapping " f^- " ρ bands. The curve on the cross-hatched data of Fig. 6(b) is a fit of polynomially modified phase space to the data.

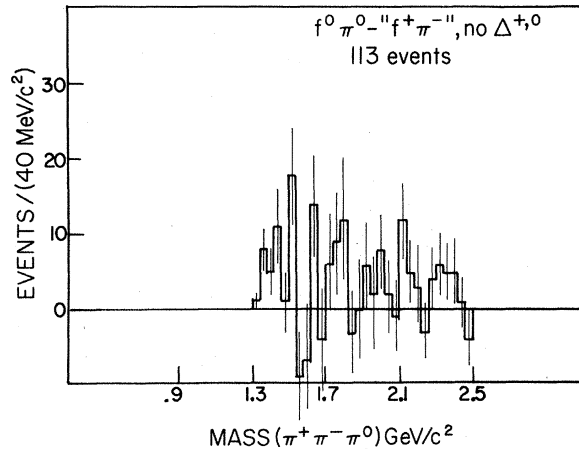


FIG. 7. The $m(\pi^+\pi^-\pi^0)$ distribution obtained by subtracting Fig. 6(a) from Fig. 6(b). As explained in the text, Sec. V, this distribution is expected to be the "true" $f^0\pi^0$ mass distribution.

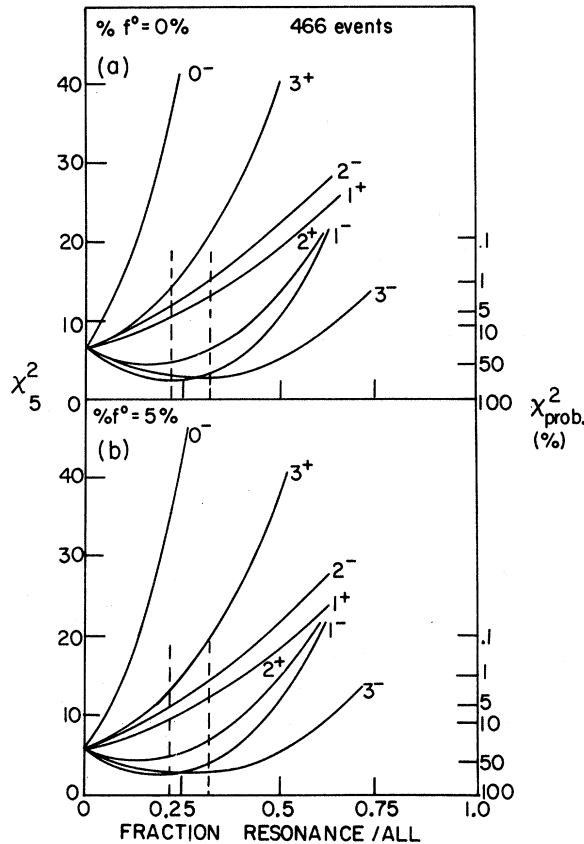


FIG. 8. One-parameter χ^2_{NDF} curves for the Dalitz-plot fits to the data in the $\phi(1680)$ mass band (see Sec. VII). The dashed lines are 1-standard-deviation limits from our determination of the "fraction of resonance/total No. of events" in this data. The spin-parities J^P are marked next to the appropriate curves. The isospin of the $\phi(1680)$ was assumed to be 0 for this analysis. (a) The percentage " f^0 /total number of events" in the data was set to 0.0%. (b) The same as (a) but with the fraction of f^0 set to 5%, our estimation of the amount of f^0 as discussed in Sec. V.

The $\cos\beta$ distribution of the normal to the 3π decay plane in the Jackson frame⁹ will be presented and compared with a restricted set of spin-parity assignments for the $\phi(1680)$.

A spin-parity analysis of the $\phi(1680)$, assuming the isospin was 0, was discussed in Ref. 8 following the techniques of Zemach²⁶ and Frazer, Fulco, and Halpern.²⁷ Dalitz-plot fits to data in the ρ bands were made for spin-parity assignments $J^P = 0^-, 1^+, 2^+, 3^+$.²⁸

The data in the 3π mass regions near the $\phi(1680)$ were divided into three regions: two control regions, $1.44 < m(3\pi) < 1.54$ GeV and $1.82 < m(3\pi) < 1.92$ GeV, and the $\phi(1680)$ mass band $1.58 < m(3\pi) < 1.78$ GeV. The background in the $\phi(1680)$ mass band was assumed to be described by the data in

the control regions. To determine the composition of this background, the control regions were fitted to an incoherent sum of 3π , $\rho\pi$, and $f^0\pi^0$ distributions, and the χ^2 was minimized. The amount of $f^0\pi^0$ and $\rho\pi$ in the background was constrained to be consistent with the fits discussed in Sec. V to the $\pi\pi$ mass distributions of Fig. 5. The contributions so determined were $f^0\pi^0/(f^0\pi^0 + 3\pi + \rho\pi) = (5 \pm 5)\%$ and $\rho\pi/(\rho\pi + 3\pi) = (60 \pm 10)\%$. These ratios then fixed the form of the background amplitude to be used in the $\phi(1680)$ mass band.

One-parameter χ^2 fits were made to the data in the $\phi(1680)$ mass band by varying the fraction of resonance to background. Individual fits were made for " $f^0\pi^0$ /all" ratios of 0 and 5% and for two bin sizes. The results of the fits to the data using different binning were essentially identical; the larger bin size allows better statistics, however, and will be presented here.

The χ^2 curves for 0 and 5% " $f^0\pi^0$ /all" ratios are shown in Fig. 8. The ratio of the amount of resonance to the total number of events in the $\phi(1680)$ mass region was determined to be $(27 \pm 5)\%$, as discussed in Sec. III. These one-standard-deviation limits are dashed on the χ^2 graphs in Fig. 8.

The natural-spin-parity assignments for the $\phi(1680)$ yield χ^2 probabilities of about 50% at the center of the resonance band as shown in Fig. 8.²⁹ The spin-parities in the unnatural series all yielded χ^2 fit probabilities $< 10\%$. The spin-parities 0^- and 3^+ can probably be excluded for the $\phi(1680)$, having χ^2 fit probabilities $< 1\%$.

The amplitudes used to describe the $\phi(1680)$ Dalitz-plot distribution were compared to the data in the two control regions to determine whether the natural-spin-parity amplitudes were favored in the entire mass region $1.44 \leq m(3\pi) \leq 1.92$ GeV. The χ^2 curves from this analysis are shown in Fig. 9. These results confirm the previous determination of the composition of the background. The unnatural spin-parities $J^P = 1^+, 2^-$ are seen to yield distributions that most nearly describe the data in control regions, whereas the spin-parities $J^P = 1^-, 2^+, 3^-$, favored in the $\phi(1680)$ region, yield poor fits to the data in control regions.

The present analysis disagrees with a previous spin-parity determination for the $\phi(1680)$ ² that favored an unnatural-spin-parity assignment. Both analyses^{2,8} have alternate fits in the conjugate spin-parity sequence with χ^2 fit probabilities of $\sim 10\%$. This disagreement is, therefore, not statistically very significant. We note, however, that while the present analysis does not strongly exclude spin-parities $1^+, 2^-$, a completely consistent description of the data in the $\phi(1680)$ and neighboring control regions is obtained for spin-parity assignments of $1^-, 2^+, 3^-$ for the $\phi(1680)$.

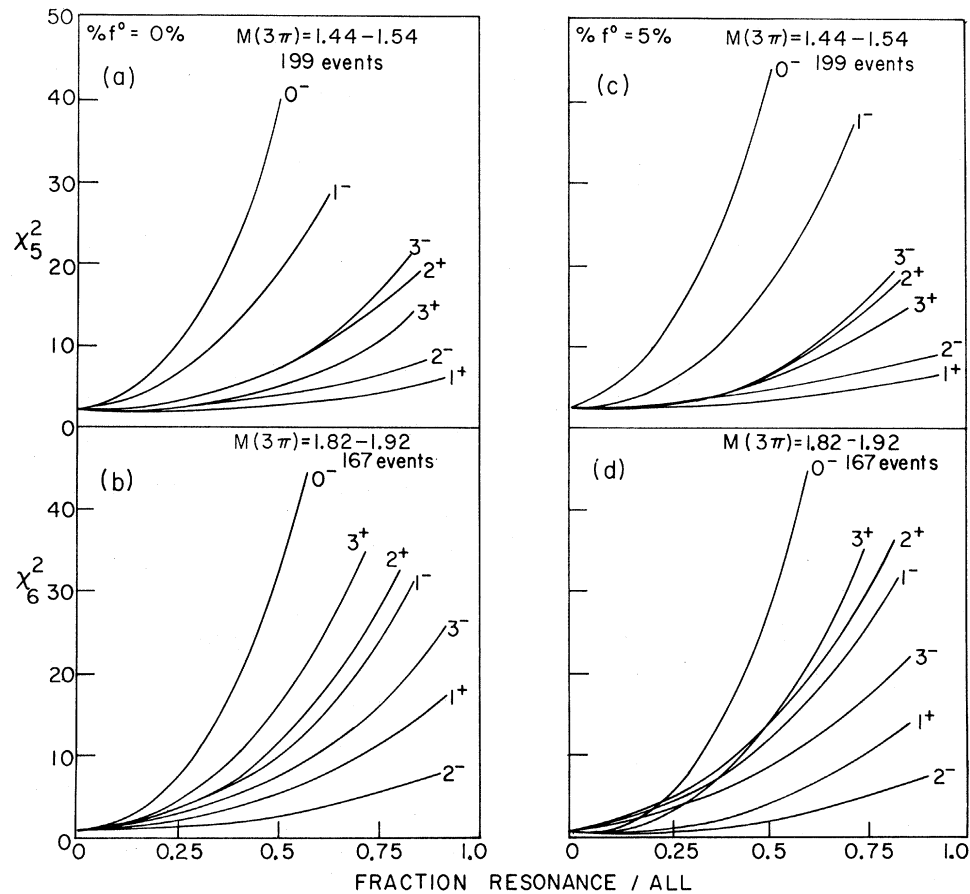


FIG. 9. One-parameter χ_{NDF}^2 curves obtained by comparing the Dalitz-plot model distributions used for the $\phi(1680) \rightarrow \rho\pi$ to the Dalitz-plot distributions for data in the control regions below and above the $\phi(1680)$. (a) $1.44 \leq m(3\pi) \leq 1.54$ GeV/c^2 . (b) $1.82 \leq m(3\pi) \leq 1.92$ GeV/c^2 , and fraction f^0/total number of events = 0%. (c) and (d) same as (a) and (b), except fraction f^0/all = 5%.

The distribution of the events in $\cos\beta$ (β is the angle between the normal to the 3π decay plane and the incident pion direction evaluated in the 3π rest frame) is shown in Fig. 10 for two sets of data at the $\phi(1680)$. These distributions were obtained by subtracting the combined $\cos\beta$ distributions from the two background regions, $1.44 \leq m(3\pi) \leq 1.54$ GeV and $1.82 \leq m(3\pi) \leq 1.92$ GeV , from the $\cos\beta$ distribution in the $\phi(1680)$ band $1.58 \leq m(3\pi) \leq 1.78$ GeV .

These distributions have Δ^{+0} events excluded. The exclusion of Δ^{+0} , as discussed in Sec. III, was not expected to distort the $\cos\beta$ distribution significantly. The data without Δ^{+0} exclusion are shown dashed in Fig. 10. With the large statistical uncertainties it is not clear that the two distributions are significantly different.

The solid curves on Fig. 10 result from fitting the expressions for $\cos\beta$ from Refs. 30 and 31, assuming spin-parities of 1^- , 2^+ , 3^- for the $\phi(1680)$. The fits shown in Fig. 10 and tabulated in Table I were all one-parameter fits, apart from an

over-all normalization to the total number of events. For spins 2^+ , 3^- , it was assumed that $\rho_{mm} \approx 0$ for $m \geq 2$.³² Fits were also made, however, with $\rho_{22} = 0.1$, and the results are included in Table I.

The $J^P = 3^-$ angular distribution contained, in addition to the production density-matrix elements of the $\phi(1680)$, an additional relative coupling of the $\phi(1680)$ to $\rho\pi$ states with different spin quantizations with respect to the normal to the 3π plane.³⁰ This parameter was evaluated using the phenomenological matrix elements of Zemach²⁶ assuming a pure $I=0$, $\rho\pi$ decay of the $\phi(1680)$. In the notation of Ref. 30, $R_0^+/(R_0^+ + R_2^+)$ was determined to be ~ 0.6 . Fits to the $\cos\beta$ distribution using this ratio as a free parameter yielded values consistent with the model calculation. The ratio was fixed, therefore, to the value 0.6 in all fits reported in Table I.

Due to the large statistical uncertainties in the data, all spin-parities attempted yielded fits with acceptable χ^2 probabilities. Summarizing Table I,

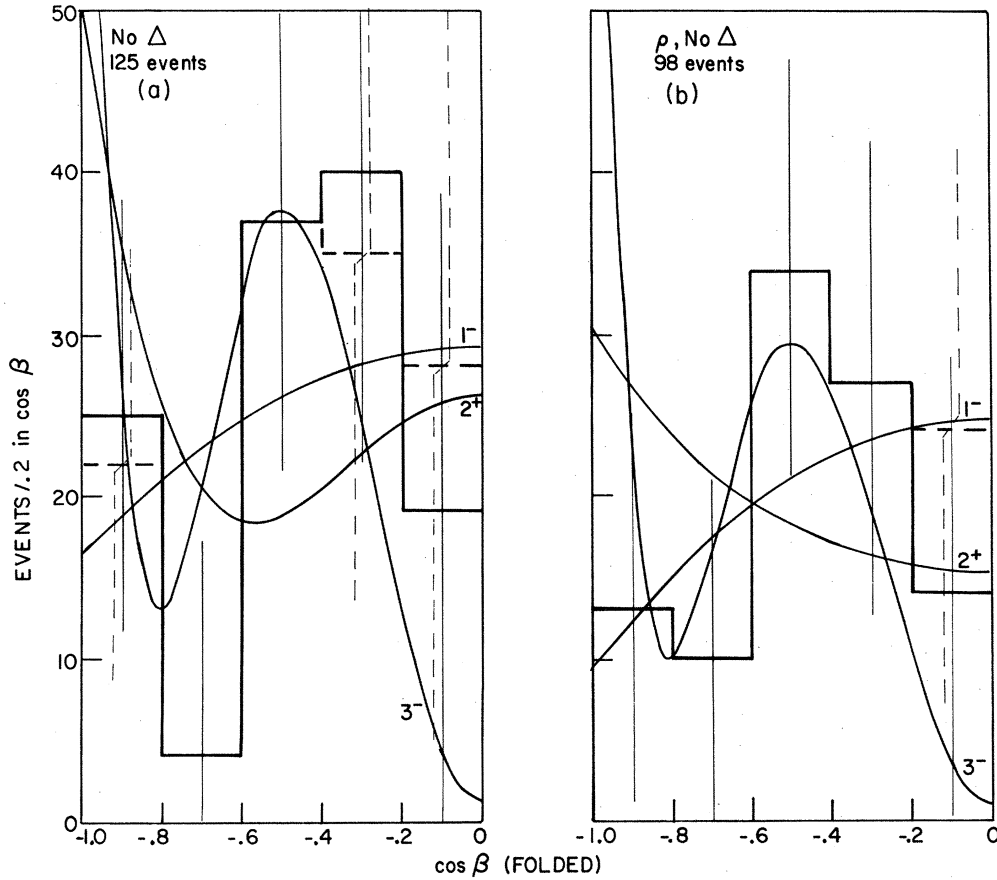


FIG. 10. Distribution of the cosine of the azimuthal angle between the normal to the 3π decay plane (in the 3π rest frame) and the initial beam direction (in the standard Jackson frame). This distribution has been folded, and has had the background subtracted as discussed in the text (Sec. VI). The data are from the $\phi(1680)$ mass band. (a) Solid histogram with $\Delta^{+,0}$ events excluded; the dashed histogram uses all the data. (b) The same as (a) but with ρ selection. The curves are fits to the solid histogram assuming that the $\phi(1680)$ has natural spin-parity (see Sec. VI).

the spin-parity 1^- yields the best agreement and 2^+ the worst. With the inclusion of $\rho_{22}=0.1$, the χ^2 for $J^P=3^-$ does approach that of $J^P=1^-$, however. With the assumptions noted above, the density-matrix elements for $J^P=1^-$, 2^+ allow some unnatural-parity exchange, but are consistent to ~ 1 standard deviation with pure natural-parity " ρ " exchange.

For spin-parity $J^P=3^-$, however, a small value of ρ_{11} is favored and therefore a large ρ_{00} . This implies a large contribution from unnatural-parity exchange.³³ The energy dependence of the cross section for $\pi^+n \rightarrow \phi(1680)p$, discussed in Sec. VII, is not consistent with simple ρ Regge exchange, but implies the added contribution of a low-lying trajectory. We note that the assignment of spin-parity 3^- to the $\phi(1680)$ and a production mechanism which includes the exchange of a low-lying unnatural-parity trajectory provide a self-consistent explanation of the variation of σ with s , the decay angular distributions and the observed Dalitz-

plot distributions of the $\phi(1680)$.

VII. COMPARISON OF $\phi(1680)$ AND A_3 MESONS

As discussed in Sec. V, the $f^0\pi^0 - f^+\pi^-$ distribution was found to be consistent with having no events above a smooth background in the $A_3 - \phi(1680)$ mass region. Taking 2 standard deviations as an estimate of the upper limit on $I=1$ enhancements in this mass region yields $\sigma_{I=1 \rightarrow f^0\pi^0} < 2.5 \mu\text{b}$. Using the result that the A_3^\pm decays with a $>50\%$ probability into $f^0\pi^\pm$ (Refs. 17–19 and Ref. 34) yields a limit of A_3^0 production in the present experiment to $\sigma_{\pi^+n \rightarrow A_3^0 p} < 5 \mu\text{b}$.

The cross sections for $\phi(1680)$ (Refs. 1, 2, and 35) and A_3 (Refs. 17, 19, 20, and 36) are plotted against the experimental beam momentum in Fig. 11. These data have been fitted with a dependence of the form $\sigma = AP_{\text{lab}}^{-n}$ yielding values of n of 2.5 ± 0.5 for $\pi^+n \rightarrow \phi(1680)p$ and 0.75 ± 0.20 for $\pi p \rightarrow A_3 p$.³⁷

TABLE I. Results of one-parameter fits to the background-subtracted $\cos\beta$ distributions of the $\phi(1680)$, shown in Fig. 10, assuming natural spin-parity for the $\phi(1680)$. Only ρ_{11} was varied in these fits; ρ_{22} (assumed to be small) was set to 0.0 or 0.1. For $J^P=3^-$, we assumed that $\rho_{33}=0.0$ (see Sec. VI for details).

J^P	χ^2 (NDF=4) ^a	ρ_{11}	ρ_{22}
"No $\Delta^{+,0}$ " selection + (background subtraction)			
1^-	3.5	0.39 ± 0.10	...
2^+	4.9	0.42 ± 0.15	0.0
	4.0	0.27 ± 0.15	0.1
3^-	4.0	0.02 ± 0.1	0.0
	3.6	0.02 ± 0.1	0.1
" ρ , no $\Delta^{+,0}$ " selection + (background subtraction)			
1^-	2.1	0.42 ± 0.11	...
2^+	4.6	0.31 ± 0.16	0.0
	3.5	0.25 ± 0.16	0.1
3^-	3.2	0.02 ± 0.1	0.0
	2.7	0.02 ± 0.1	0.1

^aNDF \equiv number of degrees of freedom.

The π^+n data at 5.1 GeV/c (Ref. 1) are consistent with an upper limit on the $\pi^+n \rightarrow A_3^0 p$ cross section of $\leq 12 \mu\text{b}$. This is consistent with the present data, and yields cross sections for A_3 production in charge-exchange reactions that are suppressed by a factor > 6 over non-charge-exchange production. Assuming a simple Regge-exchange model, the value for $\alpha_{\text{eff}} \sim 0.6 \pm 0.1$ for A_3^+ production suggests a dominant Regge f^0 contribution in this energy range. These observations are consistent with the dominant $f\pi$ decay mode and weak $\rho\pi$ decay mode observed experimentally for the A_3 . Similar features may be reproducible by multi-Regge models, however.^{7, 38}

The $\alpha_{\text{eff}} \sim -0.25 \pm 0.25$ for $\phi(1680)$ production, similar to the processes $\pi^+n \rightarrow A_2^0 p$ (Ref. 11) and $\pi^+n \rightarrow \omega^0 p$ (Ref. 39), suggests that a low-lying trajectory couples strongly to the $\phi(1680)$. A similar conjecture has been used previously to explain the reaction $\pi^+n \rightarrow \omega^0 p$ where the B meson is employed.⁴⁰ In the ω^0 reaction, the $B\pi$ decay mode is below threshold. This is not the case for the $\phi(1680)$, and may suggest that the $\omega\pi\pi$ enhancements reported in Refs. 4–6 result from a $B\pi$ decay of the $\phi(1680)$.

VIII. CONCLUSIONS

The $I^G=0^-$ assignment for the $\phi(1680)$ has been confirmed by the present data. The mass and width were determined to be 1.679 ± 0.017 and

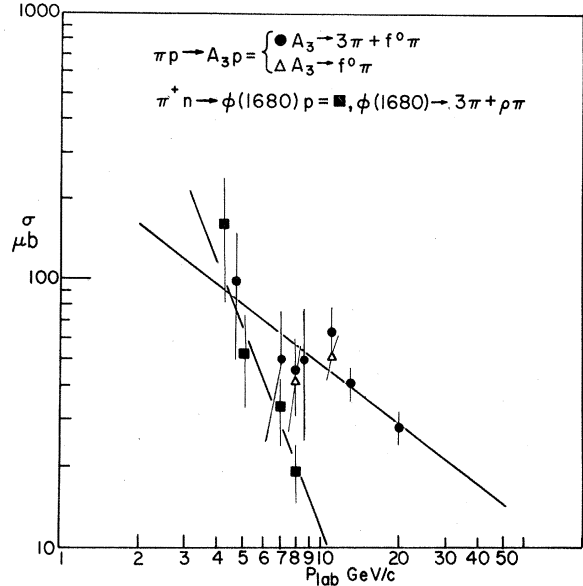


FIG. 11. Cross sections for $\pi p \rightarrow A_3 p$ and $\pi^+ n \rightarrow \phi(1680) p$. The curves are fits to this data of the form $\sigma = A P_{\text{lab}}^{-n}$ (see Sec. VII).

$0.155 \pm 0.020 \text{ GeV}$, respectively. The differential cross section for $\pi^+n \rightarrow \phi(1680) p$ [$\phi(1680) \rightarrow \pi^+ \pi^- \pi^0$] at 6.95 GeV/c was determined to be $33.5 \pm 9 \mu\text{b}$.

The differential cross section for the $\phi(1680)$, as determined by background subtraction, was consistent with a flat or decreasing t dependence in the forward direction, similar to reactions such as $\pi^+n \rightarrow \omega^0 p$ and $\pi^+n \rightarrow A_2^0 p$.

The decay of the $\phi(1680)$ is consistent with a 100% $\rho\pi/(\rho\pi + 3\pi)$ decay rate, but could not exclude a branching ratio of $[\phi(1680) \rightarrow 3\pi]/[\phi(1680) \rightarrow (3\pi + \rho\pi)] < 30\%$.

The energy dependence of the reaction $\pi^+n \rightarrow \phi(1680) p$ was found to be adequately described by $\sigma_{\pi^+n \rightarrow \phi(1680) p} \propto P_{\text{lab}}^{-2.5 \pm 0.5}$ which is inconsistent with simple ρ Regge-exchange predictions.

The spin-parity analysis of the $\phi(1680)$ favors a natural-spin-parity assignment for $J \leq 3$, although $J^P = 1^+, 2^-$ cannot be rigorously excluded.

The mass and the favored natural-spin-parity assignment for the $\phi(1680)$ suggest that it may be the Regge recurrence of the ω^0 meson.

ACKNOWLEDGMENTS

It is a pleasure to thank the operating staff of the ANL-MURA 30-in. bubble chamber and the ZGS. The efforts of the cooperative and hard-working Toronto and Wisconsin scanning and measuring staff are greatly appreciated.

*Supported in part by the National Research Council of Canada and the United States Atomic Energy Commission.

†Appreciates the support of the National Research Council of Canada and Gulf Oil Canada Limited for the period of this research.

¹N. Armenise, B. Ghidini, V. Picciarelli, A. Romano, A. Forino, R. Gessaroli, L. Lendinara, G. Quareni, A. Quareni-Vignudelli, A. Cartacci, M. Dagliana, G. diCaporiacco, G. Parrini, M. Barrier, J. Laberrigue-Frolow, and J. Quinquard, *Phys. Letters* **26B**, 336 (1968).

²I. Kenyon, J. Kinson, J. Scarr, I. Skillicorn, H. Cohn, R. McCulloch, W. Bugg, G. Condo, and M. Nussbaum, *Phys. Rev. Letters* **23**, 146 (1969).

³Particle Data Group, *Phys. Letters* **33B**, 1 (1970).

⁴J. Danysz, B. French, and V. Simak, *Nuovo Cimento* **51A**, 801 (1967).

⁵G. Yost *et al.*, cited by B. French, in *Proceedings of the Fourteenth International Conference on High-Energy Physics, Vienna, 1968*, edited by J. Prentki and J. Steinberger (CERN, Geneva, 1968).

⁶V. Barnes, S. Chung, R. Eisner, E. Flaminio, P. Guidoni, J. Kinson, and N. Samios, *Phys. Rev. Letters* **23**, 142 (1969).

⁷C.-Y. Chien, in *Meson Spectroscopy*, edited by C. Baltay and A. Rosenfeld (Columbia Univ. Press, New York, 1970).

⁸J. Matthews, J. Prentice, T. Yoon, J. Carroll, M. Firebaugh, and W. Walker, *Lett. Nuovo Cimento* (to be published).

⁹J. Jackson, *Nuovo Cimento* **34**, 1644 (1964).

¹⁰The fitting procedure used phase-space distributions composed of (a) 20% $\rho\pi$, 80% 3π phase space for the fits to the 3π mass distributions, and (b) 40% $\rho\pi$, 60% 3π phase space for the fits to the 3π mass distributions having ρ selection. The use of $\rho\pi$ phase space was suggested by the rapid rise in the 3π cross section near $m(3\pi) = 1.0$ GeV and the strong $\rho^{+\,0}$ production in the data (not shown).

¹¹J. Carroll, M. Firebaugh, A. Garfinkel, R. Morse, B. Oh, W. Robertson, W. Walker, J. Matthews, T. Johnston, J. Prentice, and T. Yoon, *Phys. Rev. Letters* **25**, 1393 (1970).

¹²I. Butterworth, J. Brown, G. Goldhaber, S. Goldhaber, A. Hirata, J. Kadyk, B. Schwarzschild, and G. Trilling, *Phys. Rev. Letters* **15**, 734 (1965).

¹³See, for example, N. Armenise, B. Ghidini, V. Picciarelli, A. Romano, A. Silvestri, A. Forino, R. Gessaroli, L. Lendinara, A. Quareni-Vignudelli, A. Cartacci, M. Dagliana, G. diCaporiacco, M. Barrier, D. Mettel, and J. Quinquard, *Nuovo Cimento* **65A**, 637 (1970).

¹⁴See, for example, N. Armenise *et al.*, Ref. 13.

¹⁵This approach is often used in studying the A_2^+ ; see, for example, G. Ascoli, H. Crawley, U. Kruse, D. Mortara, E. Schafer, A. Shapiro, and B. Terrault, *Phys. Rev. Letters* **21**, 113 (1968).

¹⁶W. Katz, T. Ferbel, P. Slattery, and H. Yuta, *Phys. Letters* **31B**, 329 (1970).

¹⁷C. Caso, F. Conte, G. Tomasini, D. Cords, J. Diaz, P. van Handel, L. Mandelli, S. Ratti, G. Vegni, P. Daronian, A. Dauden, B. Gandois, C. Kochouski, and L. Mosca, *Nuovo Cimento* **54A**, 983 (1968).

¹⁸J. Lamsa, N. Cason, N. Biswas, I. Derado, T. Groves, V. Kenney, J. Poirier, and W. Shephard, *Phys. Rev.* **166**,

1395 (1968).

¹⁹J. Bartsch, E. Keppel, G. Kraus, R. Speth, N. Tsanos, C. Grote, K. Lanius, S. Nowak, E. Ryseck, H. Bottcher, V. Cocconi, J. Hansen, G. Kellner, U. Kruse, A. Mihul, D. Morrison, V. Moskalu, and H. Tofte, *Nucl. Phys.* **B7**, 345 (1968).

²⁰M. Ioffredo, G. Brandenburg, A. Brenner, B. Eisenstein, L. Eisenstein, W. Johnson, Jr., J. Kim, M. Law, B. Salzberg, J. Scharenguivel, L. Sisterson, and J. Szymanski, *Phys. Rev. Letters* **21**, 1212 (1968).

²¹M. Aguilar-Benitez, V. Barnes, D. Bassano, S. Chung, R. Eisner, E. Flaminio, J. Kinson, R. Palmer, and N. Samios, *Phys. Rev. Letters* **25**, 54 (1970); J. Bartsch, M. Deutschmann, G. Kraus, C. Grote, J. Klugow, W. Norvak, D. Pose, T. Besliu, V. Cocconi, P. Duinker, J. Hansen, G. Kellner, S. Matsumoto, D. Morrison, R. Stroynonski, J. Whittaker, N. Barford, P. Dorman, M. Losty, M. Mermikides, B. Buschbeck-Czapp, A. Frohlich, M. Markytan, G. Otter, and H. Wahl, *Phys. Letters* **33B**, 186 (1970).

²²A. Barbaro-Galtieri, P. Davis, S. Flatté, J. Friedman, M. Garnjost, G. Lynch, M. Matison, M. Rakin, F. Solmitz, N. Uyeda, V. Waluch, R. Windmolders, and J. Murray, *Phys. Rev. Letters* **22**, 1207 (1969); T. Ludlam, J. Sandweiss, and A. Slaughter, *Phys. Rev. D* **2**, 1234 (1970).

²³An alternative explanation for the similarity of the three " f^0 " π mass distribution comes from recent $K\rho$ experiments (Ref. 22). These data suggest that any narrow $K\pi$ mass selection yields a $K\pi\pi$ mass distribution having a threshold enhancement. The qualitative similarity between the peripheral nature of the $K\pi\pi$ production in the $K\rho$ experiments and the $\pi\pi\pi$ production in our π^+n experiment suggests that the $K\rho$ result may be of relevance to our data. We note, however, that there exists some disagreement in the interpretation of the $K\pi\pi$ data in this respect. Ref. 21.

²⁴This is consistent with "average" or "finite-energy sum rule" duality since we are considering only a small $\pi\pi$ mass interval near the mass of the f^0 .

²⁵J. Jackson, in *Les Houches Summer School on Theoretical Physics*, edited by C. DeWitt and M. Jacob (Gordon and Breach, New York, 1965).

²⁶C. Zemach, *Phys. Rev.* **133**, B1201 (1964).

²⁷W. Frazer, J. Fulco, and F. Halpern, *Phys. Rev.* **136**, B1207 (1964).

²⁸For states of natural spin-parity, the $\rho\pi$ decay amplitude can be modelled unambiguously to lowest order in the pion energies. For states of unnatural spin-parity, however, decays exist in orbital waves of $l = J \pm 1$. The present analysis assumes that the dominant decay mode of the $\phi(1680)$ proceeds through the wave of lower relative angular momentum. Indeed, fits for a spin-parity assignment of $J^P = 1^+$ for the $\phi(1680)$ yielded substantially lower values of fit χ^2 for the $l=0$ amplitude than for the $l=2$ amplitude.

²⁹Spin-parities 1^- , 3^- are favored slightly over 2^+ . The primary difference between the Dalitz-plot distributions for the natural spin-parities comes in the overlapping ρ bands. In this region $J^P = 1^-$, 3^- have a constructive interference, whereas for 2^+ it is destructive. The destructive interference is not expected to be complete for 2^+ , however, as a result of the nature of the matrix element (Ref. 26) and the effects of the experimental reso-

lution (Ref. 27).

³⁰S. Berman and M. Jacob, Phys. Rev. **139**, B1023 (1965).

³¹P. Dennerly and A. Krzywicki, Phys. Rev. **136**, B839 (1964).

³²M. Gell-Mann, M. Goldberger, F. Low, E. Marx, and F. Zachariasen, Phys. Rev. **133**, B145 (1964).

³³K. Gottfried and J. Jackson, Nuovo Cimento **33**, 309 (1964).

³⁴D. Crennell, U. Karshon, K. Lai, J. Scarr, and H. Sims, Phys. Rev. Letters **24**, 781 (1970).

³⁵H. Gordon, Ph. D. thesis, University of Illinois Report No. COO-1195-179, 1970 (unpublished).

³⁶I. Veflitsky, V. Guszavin, G. Kliger, V. Kolganov, A. Lebedev, G. Lomkazi, V. Smoljankin, A. Sokolov, and E. Sisow, Phys. Letters **21**, 579 (1966); C. Baltay, H. Kung, N. Yeh, T. Ferbel, P. Slattery, M. Robin, and H. Kraybill, Phys. Rev. Letters **20**, 887 (1968).

³⁷Cross-section uncertainties are unpublished for the A_3 data at 4.7, 7.0, and 8.5 GeV/c. For these data, one-

half of the A_3 cross section has been taken as an estimate on these uncertainties. This procedure is sufficient to define a cross section for charged A_3 production at our energy.

³⁸R. Sosnowski and A. Wroblewski, cited by O. Czyzewski, in *Proceedings of the Fourteenth International Conference on High-Energy Physics, Vienna, 1968*, edited by J. Prentki and J. Steinberger, Ref. 5.

³⁹N. Armenise, B. Ghidini, V. Picciarelli, A. Romano, A. Silvestri, A. Forino, R. Gessaroli, L. Lendinara, A. Quareni-Vignudelli, A. Cartacci, M. Daghiana, G. di-Caporiacco, M. Barrier, D. Mettel, and J. Quinquard, Nuovo Cimento **65A**, 637 (1970).

⁴⁰H. Hogassen and L. Lubatti, Phys. Letters **26B**, 166 (1968); J. Tran Thanh Van, Lett. Nuovo Cimento **3**, 678 (1970); M. Barmawi, Phys. Rev. **166**, 1857 (1968); G. Hite, thesis, University of Illinois, 1967 (unpublished); J. A. J. Matthews, J. D. Prentice, T. S. Yoon, J. T. Carroll, M. W. Firebaugh, and W. D. Walker, Phys. Rev. Letters **26**, 400 (1971).

Observation of the d^* Effect in the $\bar{p}d \rightarrow p\bar{p}\pi^+\pi^-n$ Reaction at 5.55 GeV/c

H. Braun, D. Evrard, A. Fridman, J.-P. Gerber, A. Givernaud,

R. Kahn, G. Maurer, A. Michalon, B. Schiby, R. Strub, and C. Voltolini

*Laboratoire de Physique Corpusculaire, Centre de Recherches Nucléaires de Strasbourg,
Strasbourg, France*

(Received 8 December 1970)

This experiment is based on 150 000 photographs, taken at the Zero Gradient Synchrotron with the 30-in. bubble chamber. We present results on a subsample of $p_s\bar{p}\pi^+\pi^-n$ events in which the protons stopping in the chamber do not show the characteristic nucleon-spectator behavior. The selection procedure for this sample is discussed. A strong low-mass $p_s n\pi^+$ enhancement at 2.2 GeV/c² is observed. This bump is not considered as a real resonance and is interpreted as having the same origin as the 2.2-GeV/c² $d\pi$ enhancement observed, for instance, in the $\bar{p}d \rightarrow \bar{p}d\pi^+\pi^-$ reaction at the same energy.

I. INTRODUCTION

In this paper we present results on a subsample of events belonging to the $\bar{p}d \rightarrow p_s\bar{p}\pi^+\pi^-n$ channel. Throughout this work p_s will denote a proton stopping in the chamber while the symbol N_{sp} is reserved for a real nucleon spectator. The present data were extracted from a \bar{p} exposure made at the Zero Gradient Synchrotron with the 30-in. deuterium-filled bubble chamber. The 150 000 photographs were scanned twice for four-pronged events with at least one positive track stopping in the chamber. In this way we obtained an enriched sample of events with a proton spectator in the final state. Excluding that part of the events having the p_s laboratory momentum for $p_p \geq 0.28$ GeV/c, we should, in principle, be left with a $p_s\bar{p}\pi^+\pi^-n$ sample, allowing the study of the $\bar{p}n \rightarrow \bar{p}\pi^+\pi^-n$ reaction. As shown in Ref. 1, this

method does not give satisfactory results for the $\bar{p}d \rightarrow p_s\bar{p}\pi^+\pi^-n$ channel. For this reaction there is an important fraction of events having outgoing stopping protons which cannot be considered as proton spectators. These events will be studied in this work. Further experimental details on the present experiment can be found in Refs. 2 and 3.

II. SELECTION OF EVENTS CONTRIBUTING TO THE d^* EFFECT

Each event fitting the $\bar{p}d \rightarrow p_s\bar{p}\pi^+\pi^-n$ hypothesis was taken as a candidate for this reaction if there was compatibility between the calculated and observed bubble densities of the tracks. After resolving the ambiguity problems between the competitive hypotheses as described elsewhere¹ and applying further cuts on the missing mass squared and the χ^2 probability, we obtained 1239 events. For this sample we show in Fig. 1(a) the scatter